Sensors and Materials, Vol. 26, No. 9 (2014) 687–698
MYU Tokyo

S & M 1034

A Nonenzymatic Amperometric Glucose Sensor Based on a RuO_2/Graphene Sheet Composite Electrode

Ramin M.A.Tehrani* and Somayeh Beyzavi

Department of Chemistry, Yadegar-e-Imam Khomeini (RAH) Shahre Rey Branch, Islamic Azad University, 18155-144, Tehran, Iran

(Received January 5, 2014; accepted June 19, 2014)

Key words: glucose sensor, graphene sheet, nonenzymatic, ruthenium oxide

A nonenzymatic glucose sensor prepared from a mixture of ruthenium oxide (RuO_2) and graphene (GR) sheet as a composite paste electrode (RuO_2/GR CPE) was developed. The surface morphology and microstructure of the RuO_2/GR CPE were studied by scanning electron microscopy, transmission electron microscopy and X-ray diffraction analyses. The RuO_2/GR CPE was characterized by cyclic voltammetry, amperometry and electrochemical impedance spectroscopy. The RuO_2/GR CPE displayed a synergism between RuO_2 and GR in during the electrocatalytic oxidation of glucose in 3 M NaOH. The formations of Ru(VI)/Ru(IV) and Ru(VII)/Ru(VI) redox couples and the remarkable physical properties of GR were the reasons behind this phenomenon. The RuO_2/GR CPE had a linear response toward glucose over a concentration range of 0.1 to 22 mM with a detection limit of 5.60 ± 0.03 μM ($S/N = 3$) and a sensitivity of 78.4 μA mM^{-1} cm^{-2}. The sensor showed good stability and reproducibility.The RuO_2/GR CPE was not affected by the traditional interferents of the glucose sensor, namely, ascorbic acid and uric acid.

1. Introduction

Glucose sensors have become increasingly important nowadays, particularly in chemical and biological analyses, clinical detection, and environmental monitoring. The sensing is made possible through the oxidation of glucose in glucose sensors, mainly through (i) enzymatic and (ii) nonenzymatic reactions.[1,2] The enzymatic oxidation almost always involves the enzyme glucose oxidase (GO*x*) as the mediator. However, despite its rapid, selective, and sensitive nature, GO*x* has some drawbacks such as immobilization conditions, short lifetime and stability, slow response time and storage conditions.[2,3] It is also generally known that the enzyme is easily affected by temperature, humidity, pH, ionic detergents and toxic chemicals. An alternative method

*Corresponding author: e-mail: rmt@iausr.ac.ir

of addressing this problem is the nonenzymatic oxidation of glucose, which has some added advantages, namely, stability, simple fabrication, reproducibility and low cost.[2–4]

The catalytic oxidation of carbohydrates has been carried out in neutral, alkaline and acidic media using noble metals such as Pt,[2] Ni,[5] Cu,[6] Au[7] and their alloys, such as PtPb[8] and PtRu[9] at nanostructured sizes as oxidants. Moreover, the conducting metal oxides such as CuO[10] and RuO_2 and $RuO_2.xH_2O$[11–13] have also been utilized. As electrocatalysts for the glucose oxidation reaction, the conducting metal oxides have several advantages, such as high metallic conductivity, reduced overpotential and enhanced efficiency.[11–13] Interestingly, RuO_2, perhaps because of its high metallic conductivities, unusual stability and easier electron transfer abilities,[13,14] is mostly used for the oxidation of carbohydrates.[11–13] The unusual stability of Ru is related to several oxidation states within the potential region of the solvent (water) such as Ru(III), Ru(IV), Ru(VI) and Ru(VII).[13,14] It is noteworthy that an oxidation signal for a carbohydrate in acidic and neutral media is not possible in most nonenzymatic metallic modified carbon electrodes owing to the very high overpotentials. However, this is overcome in highly alkaline media where RuO_2 has been used as an electrocatalyst under alkaline condition.[9,12]

Recently, carbon-based nanomaterials such as graphene (GR) have been incorporated in nonenzymatic glucose sensors.[3,6] GR, in particular, has attracted considerable attention.[3,6,5–17] This is due to its unique physical and chemical properties, such as extremely large surface area (~2600 m^2 g^{-1}), excellent electrical and thermal conductivities, high chemical stability, fast electron transport, good mechanical strength and higher sensitivities than the traditional carbon-based electrodes.[15,16] Nonenzymatic glucose sensors based on composites of GR with Cu,[6] Ag[16] and CuO[17] have been prepared. Additionally, RuO_2/carbon[11] and RuO_2/MWCNT[18] composite paste electrodes have been used for the catalytic oxidation of glucose. Recently, a RuO_2/ GR hybrid material for a high-performance electrochemical capacitor has also been reported.[19] However, there is no report yet on the use of a composite of GR sheets with RuO_2 for glucose sensing in highly alkaline media. In this study, the combination of GR and RuO_2 as a composite paste electrode (CPE) is investigated for the development of an amperometric nonenzymatic glucose sensor in highly alkaline media.

2. Experimental

2.1 *Chemicals and equipment*

D-glucose, L-ascorbic acid (AA), uric acid (UA), D-fructose, D-galactose, mineral oil and ruthenium oxide were purchased from Sigma-Aldrich, USA. Cyclic voltammetric measurements were carried out with an Ivium potentiostat (Ivium Technologies, Eindhoven, Netherlands). Electrochemical impedance spectroscopy (EIS) measurements were carried out on Potentiostat/Galvanostat Model 273A complete with the Power Suite program (EG&G, Princeton Applied Research, USA). The analysis of EIS's results was carried out with the ZSimpWin 3.22 software (EG&G, Princeton Applied Research, USA). A three-electrode system was used in the experiment with a Pt wire as a counter electrode, Ag/AgCl (3M KCl) as a reference electrode and RuO_2/GR CPE, GR paste electrode (GR/PE) and RuO_2 paste electrode (RuO_2/PE) as working electrodes. Human blood serum samples were kindly provided by a local hospital (Pars, Iran). All experiments were performed at room temperature and in 3M NaOH.

Powder X-ray diffraction (XRD) studies of RuO_2/GR were performed with a high-resolution XRD (HR-XRD) model PANalytical (X'pert Pro, Netherlands) at 40 kV and 30 mA using a Cu Kα radiation (λ = 1.54056 Å) filter in the 2θ range from 15 to 80°. The surface morphology of the electrode was determined using field-emission scanning electron microscopy (FE-SEM) (model S-4800; Hitachi, Japan) and transmission electron microscopy (TEM) (model CM12; Phillips, Netherlands) using 80 kV.

2.2 *Preparation of GR sheets*

Graphite oxide (GO) was prepared according to the Staudenmaier method.[20] A conical flask equipped with a magnetic stir bar was filled with sulfuric acid (88 mL) and nitric acid (45 mL) and cooled by immersion in an ice bath. The acid mixture was stirred and allowed to cool for 15 min, and graphite (325 mesh, > 99.99%, Sigma-Aldrich, 5 g) was added under vigorous stirring to avoid agglomeration. After the graphite powder was well dispersed, potassium chlorate (55 g) was added slowly over a period of 15 min to avoid sudden increases in temperature. The reaction flask was loosely capped to allow gas evolution from the reaction mixture and stirred for 96 h at room temperature. Upon completion of the reaction, the mixture was poured in 4 L of deionized water and filtered. The GO was dispersed and washed in 5% HCl. GR sheets were prepared by thermal and reduction exfoliation of GO at 1050 °C in argon atmosphere and cooled in a furnace.[21]

2.3 *Fabrication of RuO_2/GR CPE*

The RuO_2/GR CPE was prepared firstly by hand mixing of GR and RuO_2 powder at a ratio of 70:30 (w/w) with an appropriate amount of mineral oil. The homogenous paste was packed into a cavity of a Teflon tube (4 mm internal diameter). Electrical contact was provided through a copper wire connected to the paste. The electrode surface was renewed by slicing out a small portion of the tube near the old surface.

3. Results and Discussion

3.1 *Structural characterization of RuO_2/GR*

The HR-XRD patterns of the RuO_2/GR composite, RuO_2 and GR sheet are shown in Fig. 1(e). For the RuO_2/GR composite, the two major peaks at 28.0 and 35.0° in the range of 20–40° are assigned to the diffraction of the {1 1 0} and {1 0 1}planes of RuO_2 with a tetragonal lattice rutile phase. This is in agreement with the RuO_2 in the JCPDS powder diffraction pattern (00-040-1290) and the parameters of the RuO_2/carbon nanocomposite,[22] RuO_2/MWCNT composite[18] and RuO_2[23] electrodes. The peaks at 25° {0 0 2} and 43° {1 0 1} are attributed to the diffraction of GR.[24] The XRD patterns of GR and RuO_2 also confirm the assignments of these peaks.

The morphologies of the as-prepared RuO_2/GR composite, GR and RuO_2 were also characterized using FE-SEM and TEM. As shown in Fig. 1(c), a large amount of the white RuO_2 particles are observed on the GR sheets. It can be clearly seen in the SEM images of the composite that RuO_2 particles are dispersed throughout the GR matrix. The SEM images of the GR sheets [Fig. 1(a)] and RuO_2 [Fig. 1(b)][18] are also shown for comparison. The TEM analysis [Fig. 1(d)] also confirms the findings. The RuO_2 particles (dark spots) appear to be distributed homogeneously throughout and adhered to the transparent GR sheet. These results clearly show the existence of $RuO_2$and GR in the CPE.

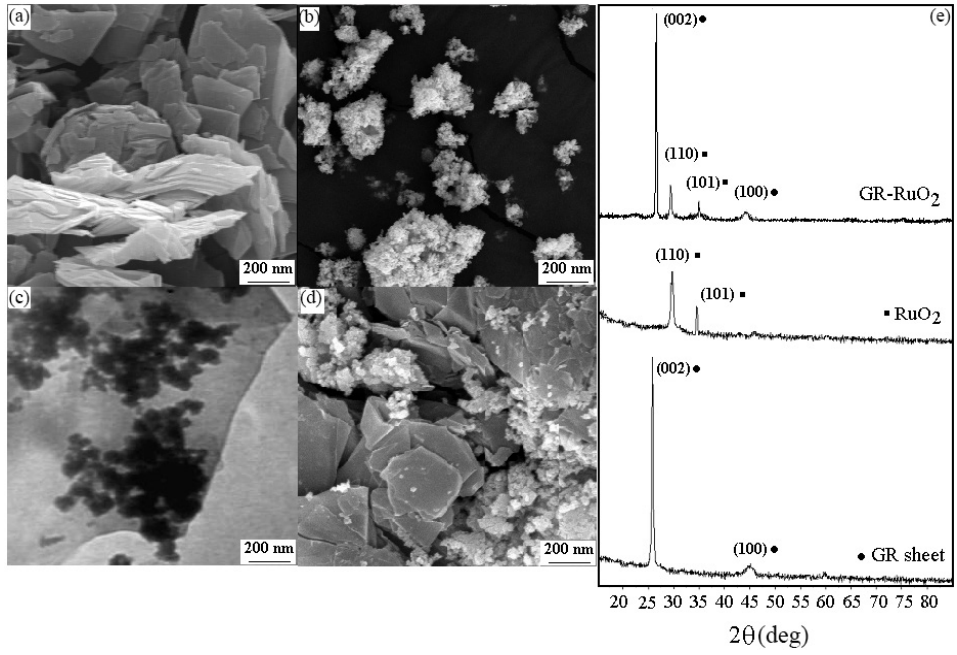

Fig. 1. FE-SEM images of (a) GR, (b) RuO_2,[18] and (c) RuO_2/GR, and (d) TEM image of RuO_2/GR composite electrode. (e) HR-XRD patterns of RuO_2/GR, RuO_2, and GR sheets.

3.2 *EIS of RuO_2/GR CPE*

EIS is performed to determine the kinetic and surface characteristics of the electrodes. Figures 2(a) and 2(b) are the respective Nyquist and Bode plots of 5 mM $[Fe(CN)_6]^{3-/4-}$ at GR/PE, RuO_2/PE and RuO_2/GR CPE within the frequency range of 100 kHz to 100 mHz at the formal potential of the redox probe. According to the standard complex function representation, the ac impedance (Z) can be described as a real (Z') part and an imaginary part (Z'') in eq. (1):

$$Z(\omega) = Z'(\omega) + jZ''(\omega) \tag{1}$$

and

$$Z''(\omega) = -1/\omega C \tag{2}$$

where $\omega = 2\pi f$ (f = frequency), $j = \sqrt{-1}$, and C = capacitance.

Usually, an almost straight line of the plot implies low transfer resistance and good conductivity of the redox probe.[6,25] As can be seen in the EIS of RuO_2/PE [Fig. 2(a), (i)] and GR/PE [Fig. 2(a), (iii)], a nearly straight line at low frequencies is observed, indicating Warburg impedance and the diffusion-limiting step of the electrode process,[3,6]

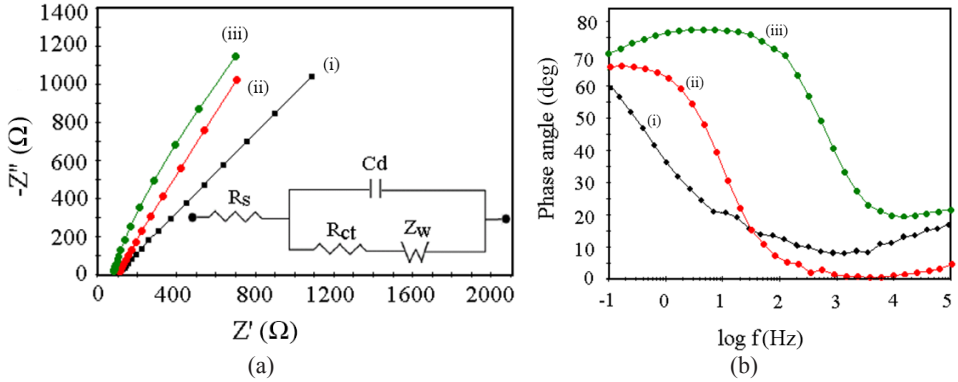

Fig. 2. (Color online) (a) Nyquist and (b) Bode plots of (i) RuO_2/PE, (ii) RuO_2/GR CPE, and (iii) GR/PE in 0.5 M KCl electrolyte solution containing 5 mM $Fe(CN)_6^{3-/4-}$. Inset (a): Randles equivalent electrical circuit for the system.

which could possibly be due to the good conductivity of the electrode materials. The loading of the RuO_2 significantly increases the conductivity of the composite[23] [Fig. 2(a), (ii)]. The imaginary part of the impedance of the RuO_2/GR CPE has a much lower value than those of the RuO_2/PE and GR/PE. It is suggested that the RuO_2-GR modified electrode maintains the good conductivity of RuO_2/PE and GR/PE. In the high-frequency region by fitting the data [inset of Fig. 2(a)], the surface electron transfer resistances (R_{ct}) of the different electrodes are as listed in Table 1. The RuO_2/GR CPE shows that the R_{ct} value is lower than those of RuO_2/PE and GR/PE, indicating an easy electronic transport at the electrode surface interface. The apparent electron transfer rate constant k_{app} is also calculated using eq. (3):[18]

$$k_{app} = RT / F^2 R_{ct} C, \tag{3}$$

where R is the gas constant (8.314 J $mol^{-1}K^{-1}$), T is the absolute temperature of the system (298 K), F is the Faraday constant (96485 C mol^{-1}), and C is the concentration of $[Fe(CN)_6]^{3-}$ (in mol/L, the concentrations of $[Fe(CN)_6]^{3-}$ and $[Fe(CN)_6]^{4-}$ are equal). The calculated k^0 value of the RuO_2/GR CPE (Table 1) is approximately ten times higher than those of RuO_2/PE and GR/PE. This indicates that the RuO_2/GR CPE has a much easier electron transfer than the others. Moreover, the Warburg region of the Nyquist plot of the RuO_2/GR CPE indicates a short and equal diffusion path length of the ions in the electrolyte. Figure 2(b) shows single-phase angle maxima at all electrodes corresponding to one relaxation process of the electrode/solution interface. The RuO_2/GR CPE [Fig. 2(b), (ii)] and RuO_2/PE [Fig. 2(b), (i)] have approached the maximum at 0.1 Hz, 66.45 and 59.90°, respectively, where the maximum for GR/PE [Fig. 2(b), (iii)] is 77.51° at 2.8 Hz. The mid-frequency region provides the interfacial layer of electrodes (ii) and (iii) as capacitors rather than as resistors as in the high- and low-frequency regions. However, at lower frequency, the capacitive behavior of the RuO_2/GR CPE is improved as compared

Table 1
Summary of estimated EIS parameters obtained for modified and unmodified electrodes.

Electrodes	R_{ct}/kΩcm^2	K_{app}/cms^{-1}
GR/PE	14.53	5.56×10^{-5}
RuO_2/PE	0.743	7.16×10^{-5}
RuO_2/GR CPE	0.101	5.26×10^{-4}

with those of GR/PE and RuO_2/PE. This shows that GR does not alter the thicknesses of the double layer (interfacial layer) surrounding the electrode. However, the most important is the existence of RuO_2, which has improved the surface characteristic of the RuO_2/GR CPE. It is also noticeable that the dispersion of RuO_2 particles over GR allows the metal oxide to be available for the electrochemical and catalytic reactions and improves the efficiency of the composite electrode.[23] The result indicates that the RuO_2/GR CPE has a higher charge transfer rate and electroactive surface area, leading to high conductance as compared with RuO_2/PE and GR/PE.

3.3 *Electrocatalysis of glucose at RuO_2/GR CPE*

The electrocatalytic properties of GR/PE, RuO_2/PE, and RuO_2/GR CPE are investigated by cyclic voltammetry in 3 M NaOH with and without glucose. The cyclic voltammogram (CV) in Fig. 3(a), (ii) illustrates that in the presence of glucose, GR/PE has no obvious electrocatalytic activity towards the oxidation of glucose. Similar results are obtained for the nonenzymatic glucose sensor using the GR electrode in alkaline media.[6,26] The increase in current response to above 600 mV in both CVs (a) and (b) is attributable to the electrochemical reaction of water, which happens at the electrode.[6] The CV at RuO_2/PE in 3 M NaOH [Fig. 3(b), (iii)] shows two pairs of redox peaks[18] at −22 to 300 mV(A1/C1) and 330 to 590 mV (A2/C2), which correspond to redox couples of Ru(VI)/Ru(IV) and Ru(VII)/Ru(VI), respectively.[11,13,18,27] With the addition of 10 mM glucose, RuO_2/PE [Fig. 3(b), (iv)] shows an increase in anodic peak currents (I_{pa}), A1' (at 360 mV) and A2' (at 620 mV), and a decrease in the related cathodic peak currents (E_{pc}). This suggests that RuO_2 catalyzes the oxidation of glucose. By comparison, two well-defined oxidation peak responses are observed for the catalytic oxidation of glucose in 3 M NaOH at the RuO_2/GR CPE. Figure 3(c), (vi) shows a significantly higher I_{pa} corresponding to both Ru(IV)/Ru(VI) (A1'' peak at 306 mV) and Ru(VI)/Ru(VI1) (A2'' peak at 585 mV), whereas the I_{pc} valves of C1'' and C2'' decrease steadily with glucose concentration. Furthermore, both A1'' and A2'' E_{pa} and C1'' and C2'' E_{pc} shifted positively, as compared with the redox peaks, A1''b and A2''b for the blank solution [Fig. 3(c), (v)]. Moreover, the I_{pa} A1'' and I_{pa} A2'' are about 5 times higher than those of the RuO_2/PE [Fig. 3(b), (iv)] and 2 times higher than the anodic peak currents in the absence of glucose at the RuO_2/GR CPE. These are indications that the oxidation of glucose in 3 M NaOH at the RuO_2/GR CPE may have occurred through surface-confined mediation by ruthenium redox species. Both ruthenate Ru(VI) (at peak A1'') and per ruthenate Ru(VII) (at peak A2'') are electroactive towards glucose oxidation.[9,13] However, as the height of the first oxidation peak is smaller than that of the second oxidation peak, different

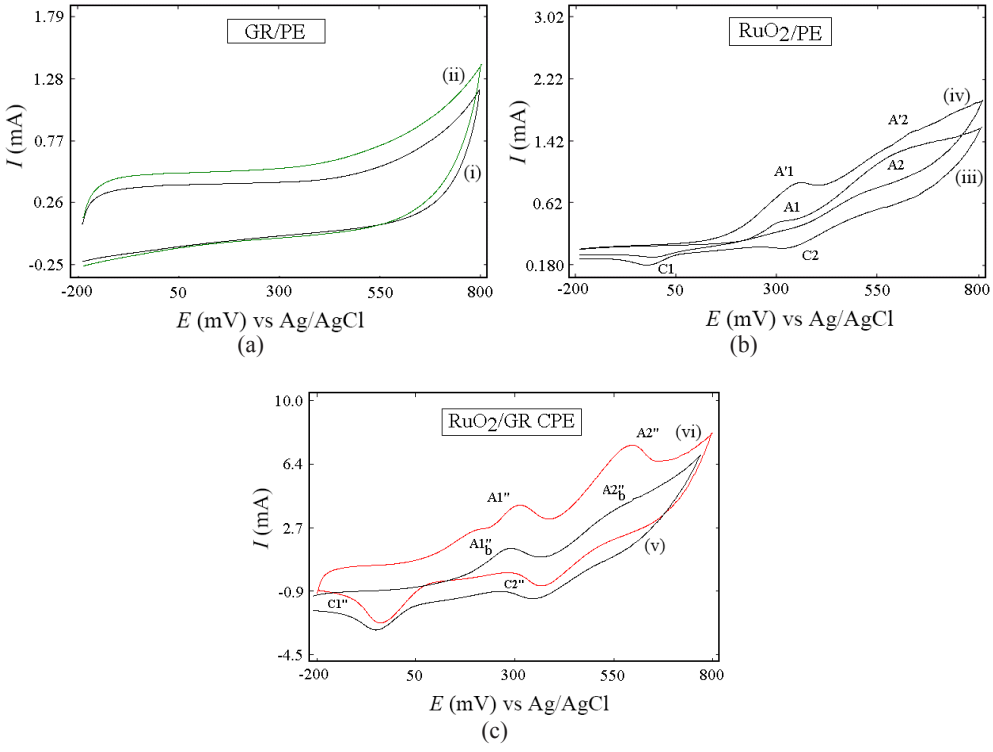

Fig. 3. (Color online) CV of 10 mM glucose in 3 M NaOH [(ii), (iv), and (vi)] and 3 M NaOH [(i), (iii), and (v)] at (a) GR/PE, (b) RuO_2/PE, and (c) RuO_2/GR CPE. Scan rate, 10 mV s^{-1}.

electrode processes might have occurred on the electrode surfaces. It is also noticeable that the nature of the catalytic species is dependent on the type of substrate material. For example, the per ruthenate [Ru(VII)] species is known to be capable of oxidizing difficult oxidizable compounds such as benzyl alcohol[28] and formic acid.[29] Also, both Ru(VI) and Ru(VII) have been used in the oxidation of formaldehyde[29] and glucose.[12,13] The pH is reported[12,13,30] to play key roles in Ru redox transitions in aqueous solution. In pH < 12, only Ru(VI) is available within the potential range in which the supporting electrolyte is stable. Ru(VII) always disproportionates to Ru(IV) and oxy/hydroxy-Ru(VI) species.[12,13] Ru(VI) is not sufficiently powerful to oxidize glucose at pH < 12.[12,30] The successive oxidation of glucose under a very strong alkaline condition (pH > 13) is shown [Fig. 3 (c), (vi)]. A stepwise mechanism similar to metal substrate electrodes[31] is then suggested for the oxidation of glucose at RuO_2/GR CPE. In this mechanism, glucose is oxidized at low potentials (A1''/C1'') that correspond to the elimination of α-hydrogen from the glucose molecule (viz. α-hydrogen lacking carbohydrates) such as sodium gluconate and fructose, followed by further oxidation at higher potentials (A2''/C2'') to produce gluconolactone.[7,13,30,32]

The schematic diagram in Fig. 4 shows the design of the RuO_2/GR CPE and the mechanism proposed earlier for the electrocatalytic oxidation of glucose in 3 M NaOH. GR with its large surface area, high conductivity and fast electron transfer has apparently enhanced the electrocatalytic performance of the RuO_2/GR CPE as compared with those of RuO_2/PE and GR/PE. RuO_2 particles dispersed on the high specific surface area of GR have shown higher electrocatalytic activity towards the oxidation of glucose while GR improves the electron transduction. This confirms the role of GR as a support for the catalyst in the composite electrode in the oxidation of glucose.[6,33] The study has revealed the synergism of both RuO_2 and GR during the oxidation.

3.4 *Voltammetric determination of glucose*

Differential pulse voltammetry of the catalytic oxidation current at different glucose concentrations was carried out. Figure 5(a) shows the differential pulse voltammogram (DPV) of 0–22 mM glucose in 3 M NaOH at the RuO_2/GR CPE. As can be seen, well-defined anodic peaks proportional to the concentration of the corresponding glucose are observed. Furthermore, I_{pa} values for both peaks A1'' and A2'' increase linearly with increasing glucose concentration, and the peak potentials shifted slightly towards the positive. The dependence of I_{pa} (based on oxidation peak A2'') on the glucose concentration is shown in Fig. 5(b). The linear regression equation is calibrated as I_p/mA = 0.2166 [glucose]/mM (mmol/L) + 4.985 with a correlation coefficient of 0.9971. The limit of detection (LOD) of glucose is 5.6 ± 0.03 μM at (S/N = 3). From the slope of the calibration plot, the sensitivity of the developed electrode is determined to be 78.4 μA mM^{-1} cm^{-2}. Table 2 shows some values of the performances of the RuO_2/GR CPE and some other nonenzymatic glucose sensors reported in the literature. It can be observed that the RuO_2/GR CPE exhibits a desirable detection limit and a wide linear range. The improvements in anodic response and LOD are due to the promoted electron transfer and facile electrocatalytic oxidation of glucose by the nanocomposite structures of RuO_2 and GR sheets, whereas the broad linear range is due to the high surface-to-volume ratio of the RuO_2/GR CPE with more electroactive sites for glucose molecules to adsorb and react.

In 10 mM glucose, a relative standard deviation (RSD) of 3.2% (n = 10) is obtained, showing good reproducibility. Good reliability is achieved using different RuO_2/GRCPEs with RSD of 4.3% (n = 6). The long-term stability of the developed electrode has been evaluated by measuring the current response of glucose within two weeks during which only 4% loss in electrooxidation capacity is observed, indicating good stability of the sensor. The decrease is assumed to have been caused by poisoning of the electrode surface via oxidative intermediates, various impurities formed and accumulated either from the electrolyte or from the surrounding atmosphere. The RuO_2/GR CPE is also incorporated in the electrochemical cell containing 10 mM glucose and 3 M NaOH to study its operational stability every day by sweeping the cyclic voltammetry (10 cycles) at a scan rate of 10 mV s^{-1} over a period of 14 d.

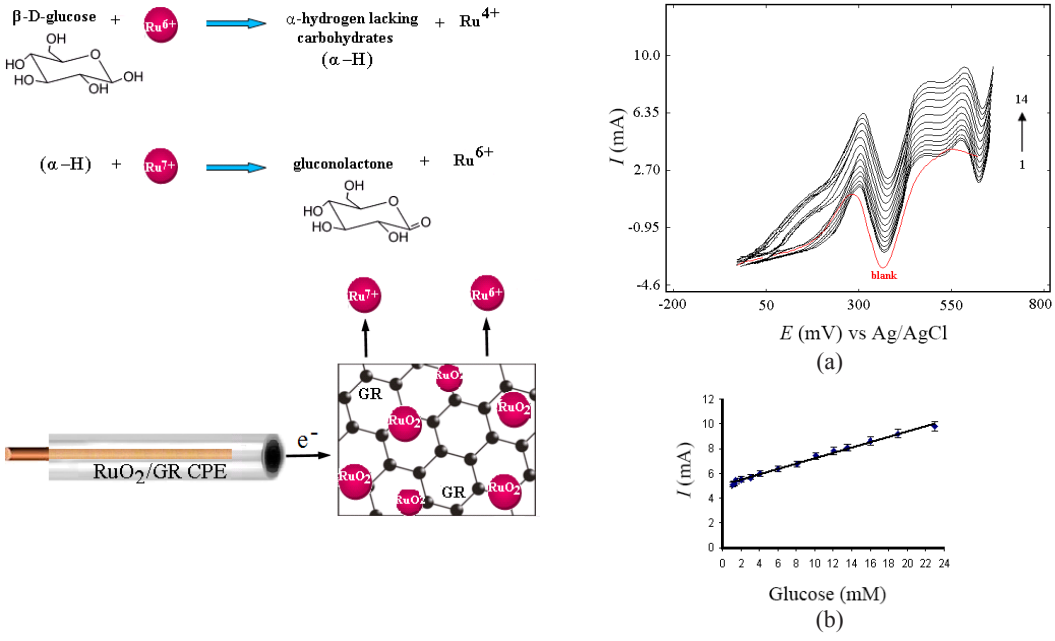

Fig. 4 (left). (Color online) Schematic diagram of the RuO_2/GR CPE and proposed mechanism for the electrocatalytic oxidation of glucose in 3 M NaOH.
Fig. 5 (right). (Color online) (a) Typical DPVs of 0.2, 0.3, 0.5, 1.0, 2.0, 3.0, 5.0, 7.0, 9.0, 11.0, 12.5, 15.0, 18.0, and 23.0 mM glucose in 3 M NaOH (1 to 14). (b) Corresponding calibration plot [each point represents the mean of three measurements (SD, ±0.03)]. Pulse amplitude 50 mV and potential step 10 mV.

Table 2
Performances of various nonenzymatic glucose sensors.

Electrodes	Applied potential (V vs Ag/AgCl)	Linear range (mM)	Detection limit (μM)	Ref.
GR (alone)	0.4	0.5−7.5	10	3
PtRu/MWCNTs	0.55	1−15	25	9
RuO_2-Prussian blue	1.1	0.3−20	40	12
CuO-GR-GCE	0.59	0.002−4	0.7	17
RuO_2/MWCNT CPE	0.5	0.5−50	33	18
Mn_2/GO	−0.3	5−600	0.8	34
CuNPs/GR	0.5	1−10	0.2	35
Pd NPs/GO	0.4	0.2−10	10	36
RuO_2/GR CPE	0.5	0−22	5.6	This work

3.5 *Interference effects*

The specificity of the sensor has been investigated using different interferents such as AA, UA, and other saccharides that normally coexist with glucose in human blood serum and other samples. The normal physiological level of glucose is 3–8 mM and the interfering species (*e.g.*, AA, UA, fructose, and galactose) are about 0.1 mM, with a glucose: interfering species ratio of more than 30:1 and is much higher in food samples.[37]

In acidic[12] and physiological[38] media, AA and UA interferents will be oxidized at the RuO_2-modified electrodes owing to the existence of powerful oxidant RuO_x species. However, the electrode processes of AA and UA are pH-dependent in solutions with pH < 10. Hence, the electrocatalytic oxidation of AA and UA is usually observed at pH 2 to 7.4. In a strong alkaline solution, I_{pa} is suppressed significantly.[39,40] In this study, the interference experiments are carried out by the successive addition of 6.0 mM glucose and 0.3 mM each of AA, UA, fructose and galactose in 3 M NaOH. Figure 6 shows the measured effects of interfering species along with glucose at +0.50 V. As can be seen, the RuO_2/GR CPE does not show any significant decline in sensor response. These results demonstrate that the RuO_2/GR CPE is highly specific towards glucose even in the presence of common interfering species normally found in food and biological samples.

3.6 *Real sample analysis*

To evaluate the applicability of the developed sensor in real samples, it is applied to determine glucose human blood serum samples. The collected human blood serum samples are diluted 25 times with 3 M NaOH and measured under optimal experimental conditions. The results of this experiment are presented in Table 3. The averaged RSD of 3.2% and accuracy of 97 to 100.5% have been obtained, suggesting the successive applicability of the proposed strategy for clinical applications.

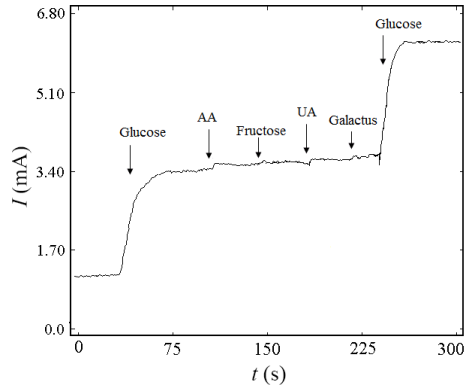

Fig. 6. Amperometric response of the interferences in 3 M NaOH at the RuO_2/GR CPE with successive addition of 6.0 mM glucose and. 0.3 mM each of AA, UA, fructose, and galactose as indicated at 500 mV.

Table 3
Determination of glucose concentration in human blood serum sample.

Sample	Measured by the hospital-used instrument (mM)	RSD (%) (n = 3)	Found by the developed sensor (mM)	RSD (%) (n = 3)	Accuracy (%)
1	3.8	2.9	3.70	2.3	97.4
2	3.6	3.1	3.65	3.9	101.5
3	4.2	3.6	4.14	2.7	98.7
4	5.6	3.2	5.63	3.6	100.5

4. Conclusions

In this study, a new amperometric nonenzymatic glucose sensor based on a RuO_2/GR CPE has been developed. The developed RuO_2/GR CPE is easily prepared. It has demonstrated greater electrocatalytic activity towards the oxidation of glucose. The incorporated GR has increased the effective electroactive surface area and electron transduction and served as an excellent matrix for the dispersed catalytic agent, RuO_2. The synergism of RuO_2 and GR has significantly enhanced the current response of glucose. The developed electrode has excellent sensitivity, reproducibility, stability and reliability in the determination of glucose. The effect of traditional interfering species, namely, AA and UA, is not significant. The analyses of simulative and real serum samples suggest that RuO_2/GR CPE is useful for routine glucose analysis in serum.

References

1 M. Liu, R. Liu and W. Chen: Biosens. Bioelectron. **45** (2013) 206.
2 K. E. Toghill and R. G. Compton: Int. J. Electrochem. Sci. **5** (2010) 1246.
3 M. Mallesha, R. Manjunatha, G. S. Suresh, J. S. Melo, S. F. D'Souza and T. V. Venkatesha: J. Solid State Electrochem. **16** (2012) 2675.
4 Y. J. Lee, J. D. Kim and J.Y. Park: J. Korean Phys. Soc. **54** (2009)1769.
5 R. M. Abdel Hameed: Biosens. Bioelectron. **47** (2013) 248.
6 J. Luo, S. Jiang, H. Zhang, J. Jiang and X. Liu: Anal. Chim. Acta **709** (2012) 47.
7 J. W. Wu, C. H. Wang, Y. C. Wang and J. K. Chang: Biosens. Bioelectron. **46** (2013) 30.
8 Y. Bai, Y. Sun and C. Sun: Biosens. Bioelectron. **24** (2008) 579.
9 L. H. Li, W. D. Zhang and J. S. Ye: Electroanalysis **20** (2008) 2212.
10 T. Soejima, H. Yagyu, N. Kimizuka and S. Ito: RSC Adv. **1** (2011) 187.
11 J. Wang and Z. Taha: Anal. Chem. **62** (1990) 1413.
12 A. S. Kumar, P. Y. Chen, S. H. Chien and J. M. Zen: Electroanalysis **17** (2005) 210.
13 V. Dharuman and K. C. Pillai: J. Solid State Electrochem. **10** (2006) 967.
14 T. P. Luxton, M. J. Eick and J. K. G. Scheckel: Colloid Interface Sci. **359** (2011) 30.
15 J. Yang and S. Gunasekaran: Carbon **51** (2013) 36.
16 Y. Zhang, S. Liu, L. Wang, X. Qin, J. Tian, W. Lu, G. Changa and X. Sun: RSC Adv. **2** (2012) 538.

17 L. Luo, L. Zhu and Z. Wang: Bioelectrochem. **88** (2012) 156.
18 R. Mohammad Ali Tehrani and S. Ab Ghani: Biosens. Bioelectron. **38** (2012) 278.
19 L. Deng, J. Wang, G. Zhu, L. Kang, Z. Hao, Z. Lei, Z. Yang and Z.-H. Liu: J. Power Sources **248** (2014) 407.
20 L. Staudenmaier: Ber. Dtsch. Chem. Ges. **31** (1898) 1481.
21 H. C. Schniepp, J. L. Li, M. J. McAllister, H. Sai, M. H. Alonso, D. H. Adamson, R. K. Prud'homme, R. Car, D. A. Saville and I. A. Aksay: J. Phys. Chem. B **110** (2006) 8535.
22 H. Kim and B.N. Popov: J. Power Sources **104** (2002) 52.
23 A.L.M. Reddy and S. Ramaprabhu: J. Phys. Chem. C **111** (2007) 7727.
24 E. Dervishi, Z. Li, F. Watanabe, A. Biswas, Y. Xu, A. R. Biris, V. Saini and A. S. Biris: Chem. Commun. **27** (2009) 4061.
25 H. Fan, Y. Li, D. Wu, H. Ma, K. Mao, D. Fan, B. Du, H. Li and Q. Wei: Anal. Chim. Acta **711** (2011) 24.
26 Y. Hu, J. Jin, P. Wu, H. Zhang and C. Cai: Electrochim. Acta **56** (2010) 491.
27 J. W. Kim and S. M. Park: J. Electrochem. Soc. **146** (1999) 1075.
28 S. M. Lin and T. C Wen: J. Appl. Electrochem. **25** (1995) 73.
29 E. J. M. O'Sullivan and J. R. White: J. Electrochem. Soc. **136** (1989) 2576.
30 J. M. Zen, A. S. Kumar and J. C. Chen: J. Mol. Catal. A: Chem. **165** (2001) 177.
31 M. V. Hsiao, R. R. Adzic and E. B. Yeager: J. Electrochem. Soc. **143** (1996) 759.
32 J. Shan Ye, Y. Wen, W. D. Zhang, L. M. Gan, G. Q. Xu and F. S. Sheu: Electrochem. Commun. **6** (2004) 66.
33 Q. Chen, L. Zhang and G. Chen: Anal. Chem. **84** (2012) 171.
34 L. Li, Z. Du, S. Liu, Q. Hao, Y. Wang, Q. Li and T. Wang: Talanta **82** (2010) 1637.
35 J. Luo, H. Zhang, S. Jiang, J. Jiang and X. Liu: Microchim. Acta **177** (2012) 485.
36 Q. Wang, X. Cui, J. Chen, X. Zheng, C. Liu, T. Xue, H. Wang, Z. Jin, L. Qiao and W. Zheng: RSC Adv. **2** (2012) 6245.
37 Z. J. Zhuang, X. D. Su, H. Y. Yuan, Q. Sun, D. Xiao and M. M. F. Choi: Analyst **133** (2008) 126.
38 J. B. Raoof, R. Ojani and M. Baghayeri: Anal. Methods **3** (2011) 2367.
39 G. Hu, Y. Ma, Y. Guo and S. Shao: Electrochim. Acta **53** (2008) 6610.
40 C. Wang, R. Yuan, Y. Chai, S. Chen, Y. Zhang, F. Hu and M. Zhang: Electrochim. Acta **62** (2012) 109.